minerals

MDPI

Article

Hydrothermal Metasomatism and Gold Mineralization of Porphyritic Granite in the Dongping Deposit, North Hebei, China: Evidence from Zircon Dating

Hao Wei [1], Jiuhua Xu [2,*], Guorui Zhang [1], Xihui Cheng [3], Haixia Chu [4], Chunjing Bian [2] and Zeyang Zhang [2]

1 Geological Testing Center, Hebei GEO University, Shijiazhuang 050031, China; ronghaiwei@163.com (H.W.); zgrsdyney@163.com (G.Z.)
2 School of Civil and Environmental Engineering, University of Science and Technology, Beijing 100083, China; bianjing0314@163.com (C.B.); wagzlxlm@163.com (Z.Z.)
3 MNR Key Laboratory of Metallogeny and Mineral Assessment, Institute of Mineral Resources, Chinese Academy of Geological Sciences, Beijing 100037, China; cheng_xihui@163.com
4 School of Earth Sciences and Resources, China University of Geosciences, Bejiing 100083, China; haixia.chu@cugb.edu.cn
* Correspondence: jiuhuaxu@ces.ustb.edu.cn

Received: 30 June 2018; Accepted: 15 August 2018; Published: 21 August 2018

Abstract: A porphyritic granite intrusion was recently discovered in the Zhuanzhilian section of the Dongping gold deposit. There is as many as one tonnage of Au in the fractured shear zone within the porphyritic granite intrusion, but no relevant reports concerning the origin and age of the intrusion has been published as yet. In this paper, zircon U-Pb dating is used to study the geochronology of porphyritic granite, in order to find out the evidence of age and the relationship with gold mineralization. There are two groups of zircon $^{207}Pb/^{235}U$-$^{206}Pb/^{238}U$ concordant ages of porphyritic granites: The concordant age of 373.0 ± 3.5 Ma, with the weighted mean age of 373.0 ± 6.4 Ma; and the concordant age of 142.02 ± 1.2 Ma with the weighted mean age of 142.06 ± 0.84 Ma. We believe that the first group might represent the age of residual zircon of alkaline complex, while the second group might be related with main gold mineralization. The obtained results of the petrography and electron probe analysis indicate that the porphyritic quartz and porphyritic granite, as well as gold mineralization, might be products of a late replacement of tectonic-hydrothermal fluid, which was rich in Si, Na and K originally and later yielded gold-forming fluids.

Keywords: porphyritic granite; zircon dating; hydrothermal metasomatism; Dongping gold deposit

1. Introduction

The gold deposits associated with alkaline rocks worldwide are widely distributed and have important economic value. Representative deposits include the US Cripple Crick Gold-Strontium Deposit and Bingham Copper-Gold Deposit; Papua New Guinea Pogel Gold deposits and Radom gold deposits; Glasgow copper-gold deposits in Indonesia and Batu-Haijiao copper-gold deposits; Katia copper-gold deposits in Australia and Skurian copper-gold deposits in Greece. In addition, the Enpaor large gold deposit in Fiji, the large copper-gold deposit in Ollumbrila, Argentina, and the Saskin-Uranium deposit in Canada are also considered to be products of alkaline magma activity [1,2]. The alkaline magmatism and related fluid activities of such deposits are the "carrier" of many large and extra-large gold deposits. For example, the ore-forming rock body of the Kadia Ridgeway

copper-gold deposit in Australia is an alkali- and potassium-rich intermediate intrusive rock. Moreover, the mineralization type of the deposit is mainly quartz vein type, and the potassium alteration is closely related to mineralization [3].

The Dongping gold deposit, located in middle northern part of the North China Craton, is the first giant gold deposit discovered among the alkaline complex-hosted in China in the 1980s. The predecessors generally believed that alkaline rock formations in the area formed in the Hercynian period [4,5]. In the 90s, the metallogenic age of the Dongping gold deposit are not uniform, Xiang et al. [6] believed that the normal lead age of the lead isotope of the ore was 127 Ma, which represents the age of gold mineralization. Song et al. [7] believed that metallogenic age was 157–177 Ma, while Li et al. [8] suggested that the age of the main mineralization period in the Dongping gold deposit was 350.9 ± 0.9 Ma. In recent years, Li et al. [5,9] used the hydrothermal zircon U-Pb dating to obtain an altered rock age of 140.3 ± 1.4 Ma, representing the metallogenic age. Since the beginning of this century, the close genetic connection between the gold deposit, and the Yanshanian potassium granite with the age of 135.5 ± 0.4 Ma [10] in the south of Dongping (Figure 1) has gradually attracted the attention of researchers [11,12]. Most people infer that the Yanshanian tectonic-magmatic activity promoted underground hydrothermal fluids to leach and extract gold and other metals from alkaline complexes and Archean Chongli group. Gold and other metals are mineralized in the favorable part of the ductile shear zone, with a suitable physicochemical environment for gold precipitation. The study of isotopic chronology also shows that the gold was mineralized in the Early Cretaceous [4,5].

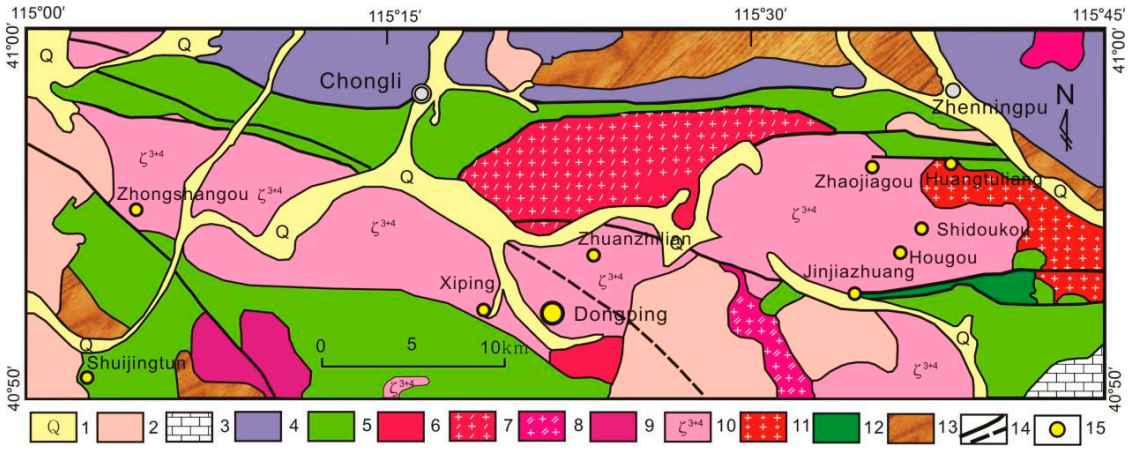

Figure 1. Simplified geological map of Shuiquangou alkaline complex in Zhangjiakou area, Hebei Province China (modified after Li et al. [5]; Song et al. [7]). (1) Quaternary; (2) Yanshanian intermediate-acidic volcaniclastic rocks; (3) Neoproterozoic and Mesoproterozoic cover rocks; (4) Paleo Proterozoic Hongqiyingzi Group; (5) Archean Chongli Group; (6) Shuiquan potassium granite; (7) Honghualiang biotite granite; (8) adamellite; (9) porphyritic granite; (10) Shuiquangou alkaline complex; (11) Hot spring giant porphyritic granite; (12) Ultramafic rocks; (13) Achaean granite gneiss; (14) faults; (15) gold deposits.

In recent years, a porphyritic granite intrusion was discovered in the Zhuanzhilian area of the Dongping Gold deposit during the peripheral exploration. Gold mineralization is intensive within the shear zone of the porphyritic granite intrusion, and Au reserves are estimated to be more than one tonnage; but no relevant research on porphyritic granite was done as yet. The age of gold mineralization in the porphyritic granite and the relations between porphyritic granite and gold mineralization are still questions. Therefore, the age of gold mineralization in porphyritic granite is needed to be clarified. And also, the natures of metasomatic fluids and their relations with porphyritic granite and gold mineralization are significant for further study of ore genesis and regional exploration.

2. Geological Background

The Dongping Gold deposit, located 12 km south to the downtown Chongli of northern Hebei Province, is tectonically in the middle part of the northern margin of the North China Craton (NCC), and at south of Shangyi-Chicheng-Damiao E-W trending deep faults (Figure 1). In the northern block of the fault, the main strata are Paleo-Proterozoic Hongqiyingzi group which is dominated by chlorite-quartz schist and biotitic granulite. While in the southern block, the strata are composed of Archean Chongli Group mainly comprising dihedral granulite and hornblende gneiss, and Neoproterozoic and Mesoproterozoic sedimentary cover rocks, and Mesozoic volcanoclastic rocks (Figure 1). The Chongli group has been affected by regional metamorphism and migmatization. There are three major NWW trending faults in the area, which are secondary faults of Chongli-Chicheng deep fault. They control the distribution of Shuiquangou alkaline complexes as well as Dongping and Hougou gold deposits. Shao et al. [13] suggested that the relatively open structure was formed in Zhangxuan area at 140 Ma or so.

The outcrop strata in the Dongping deposit are mainly the Archean Chongli amphibolite to the granulite facies metamorphic rocks [7]. The deposit is controlled by E-W striking fault and S-N trending fault which are the associated faults of the E-W striking Shangyi-Chongli-Chicheng deep fault. The ore bodies mainly occur at the junction of these two faults within Hercynian Shuiquangou alkaline complex [14]. As for the age of alkaline rock, Luo et al. [4] measured the SHRIMP zircon U-Pb age of 390 ± 6 Ma for the alkaline complex in Dongping gold deposit, and 386 ± 6 Ma for Shuiquangou syenite in Hougou gold deposit. The U-Pb average age of residual magmatic zircon in the deep potassic alteration rock vein of No. 70 is 382.8 ± 3.3 Ma from Li et al. [9], and that of magmatic zircon in K-feldspar-quartz vein of No. 1 is 380.5 ± 2.6 Ma from Li et al. [5]. The Shuiquangou alkaline complex is mainly divided into three parts: The west, the middle, and the east, with an area of about 350 km^2. The western rock section is dominated by the combination of angular syenite. The main rocks are characterized by medium-coarse grain granitic texture, porphyritic texture, massive structure with grain size of 5~15 mm; content of quartz is <3% generally, local up to 8%, K-feldspar accounts for about 50%, plagioclase (albite, oligoclase) accounts for about 20%; dark mineral content is 15~20%, mainly for hornblende and diopside. The middle section of the alkaline complex is dominated by a combination of aegirine-augite syenite. The main rocks are characterized by medium-fine grain granitic texture, massive structure with grain size of 1.5~2 mm, quartz content of 3~10%, K-feldspar (microcline, orthoclase) of 70% to 85%, plagioclase (albite, oligoclase) of 5 to 15%; generally dark minerals account for 5% to 10%, mainly diopside, aegirite, augite, etc. The eastern section of the alkaline complex is dominated by a combination of melanite syenite. The main rocks are characterized by medium-fine grain granitic texture and massive structure with grain size of 1.5~2 mm; quartz content is more than 5%, and K-feldspar accounts for 70–90%, plagioclase accounts for about 5% to 10%; generally dark minerals are 3% to 5%, mainly melanite, diopside, etc.; crushing structure and brittle-ductile shear deformation is common, accompanied by a strong metasomatism [15].

Secondly, there are Yanshanian potassium granites and middle-acidic vein. The age of the zircon LA-ICP-MS U-Pb dating for the volcanic rock of the Zhangjiakou Formation in the Zhangjiakou area is 143.0 ± 3.7 to 136.1 ± 1.4 Ma from Wei et al. [16]. A potash feldspar granite intrusion, namely Shangshuiquan orthoclase granite occurs in the south-eastern part of the mining area, which intruded along the contact zone between the Archean metamorphic rocks, and the Hercynian alkaline complex in the form of small stock. Recently, Shangshuiquan orthoclase granite intrusion has extended to Zhuanzhilian area closely related to the Dongping gold deposit, and has an exposed area of about 8 km^2 and LA-ICP-MS zircon U-Pb age of 142.9 ± 0.8 Ma from Jiang et al. [11]. Mo et al. [10] obtained a zircon U-Pb age of 135.5 ± 0.4 Ma for the single-particle zircon of Shangshuiquan potassium granite. Jiang et al. [17] obtained LA-ICP-MS zircon U-Pb ages of 142.9 ± 0.8 Ma, which are close to the age (140 ± 1.4 Ma) of Dongping gold deposit alteration rock. The dykes are widely distributed in this area, including granite porphyry, monzonite porphyry, quartz syenite porphyry, and hornblende syenite porphyry. The dark gray diorite in the eastern part of the Shuiquangou alkaline complex has

an exposed area of about 1 km^2, and the zircon SHRIMP U-Pb age is 139.5 ± 0.9 Ma [18], which is close to the metallogenic age of 140.3 ± 1.4 Ma in the Dongping gold deposit. It is closely related to the formation of the Dongping gold deposit. In summary, the tectonic-hydrothermal fluids caused by the Mesozoic magmatism activities may be the main factor for the gold mineralization.

The mineralization types include potassic altered rock and quartz vein, and the ore belt strikes NNE. The ore is dominated by gold-bearing silica-potassic altered rocks, followed by gold-quartz veins. The ore minerals in the ore are mainly pyrite, pyrrhotite, chalcopyrite, galena, stibnite, sphalerite, native gold and calaverite, and gangue minerals are quartz, K-feldspar, plagioclase, and sericite.

3. Characteristics of Porphyritic Granite

3.1. Occurrence

A porphyritic granite intrusion was discovered recently in the Zhuanzhilian area of the Dongping gold deposit, which occur as ribbon zone striking NEE-SWW with a width of 15–50 m within the Shuiquangou alkaline complex (Figure 2). The porphyritic granite is controlled by the NEE-SWW striking shear zone and intrude into the monzonite of the alkaline rock along the NEE-SWW striking shear zone. Silicification and potassiumization are relatively developed in the shear zone. An outcrop on the surface can be seen (Figure 3C). Exploratory drilling found that gold grades of altered rocks near shear zone in porphyritic granite can be up to 5.96 g/t, and generally reached 0.8~0.5 g/t, suggesting that there is a close relationship between gold mineralization and shear zones in porphyritic granite.

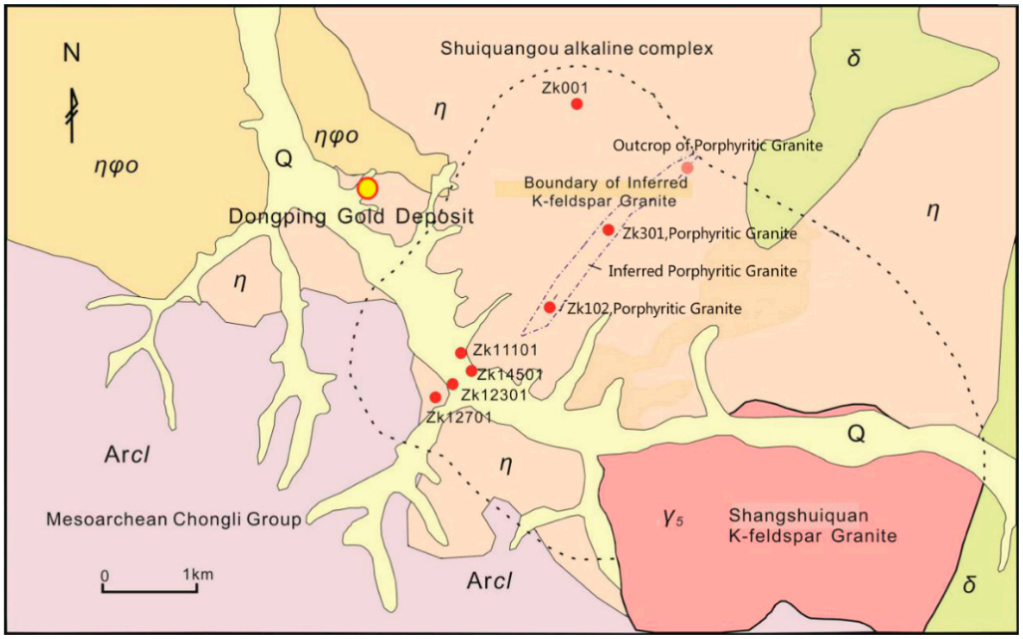

Figure 2. Sketch map of the Dongping gold deposit (after 1:10,000 geological map surveyed by Geological Exploration Report of Dongping Deposit, Chongli Zijin Mining Co., Ltd., Zhangjiakou, China, 2012). Ar*cl*, Archean Chongli group metamorphic rocks; η, Shuiquangou alkaline complex; ηφo, hornblende monzonite; γ_5, Shangshuiquan K-feldspar granite; δ, diorite.

Figure 3. Characteristics of porphyritic granite in the Dongping gold deposit. (**A**,**B**) Porphyritic quartz in the porphyritic granite with chlorite veins, ZK301A drilling; (**C**) an outcrop of the porphyritic granite on the surface, Mazhangzi.

3.2. Petrography

The petrological characteristics of porphyritic granite are: Plagioclase (~20%), K-feldspar (~55%), and quartz (~25%). Plagioclase is mainly albite and occurs as fine aggregate (0.05~0.1 mm) (Figure 4C,D). The K-feldspar seems dirty on the surface in thin section, and garnet can be seen between some grains of the K-feldspar. Quartz occurs mainly as phenocrysts or aggregates with sizes ranging from 0.5 to 10 mm. Its characteristics indicate that it is not truly phenocryst. We prefer to call them porphyritic quartz. Lenticular quartz grains with directional distribution can be seen in the fragmented porphyritic granite (Figure 4B). A single porphyritic quartz is composed of one or several quartz crystals surrounded by fine recrystallized quartz (Figure 4A). Tiny feldspar crystals and more fluid inclusions can be seen as inclusions along the growth zone or within the fracture of porphyritic quartz (Figure 4E), including liquid-vapor two-phase aqueous inclusions and, CO_2-H_2O inclusions (Figure 4F). Electron probe analysis on feldspar inclusions within porphyritic quartz was carried out by Xu et al. [19]. The results show two types of feldspar: One is identified as K-feldspar, and the other is identified as albite (Table 1). Albite and K-feldspar typically occur as stripe feldspar in one inclusion.

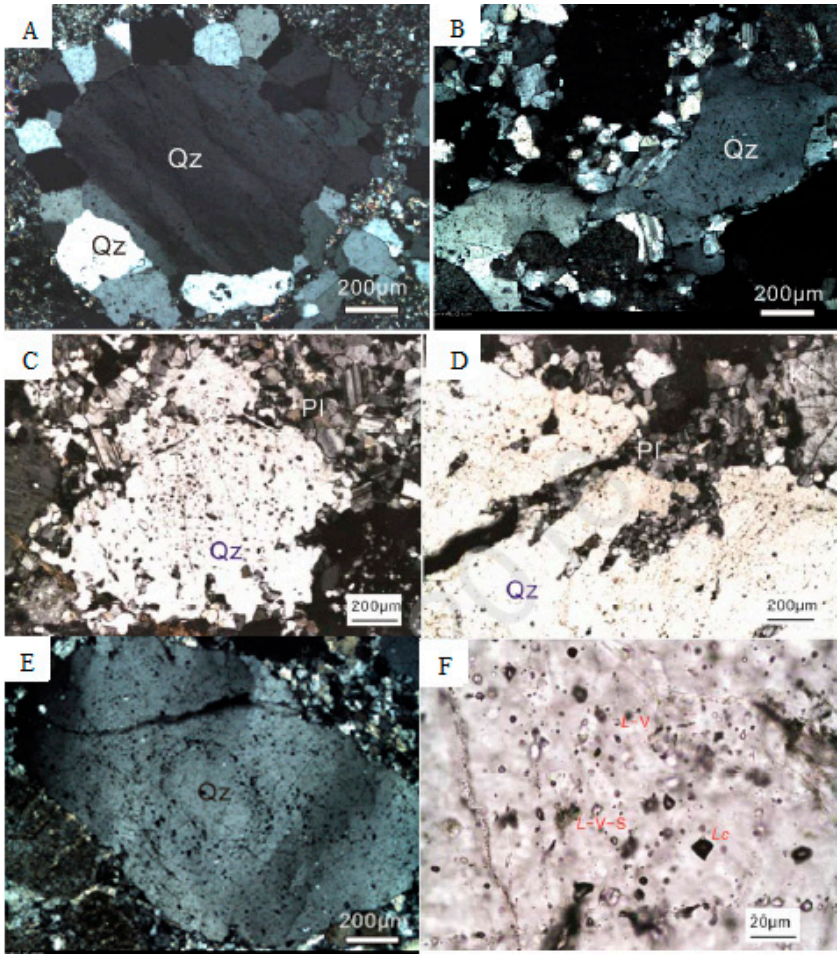

Figure 4. Microscopic features of porphyritic granite and quartz phenocryst in Dongping gold deposit. (**A**) Secondary quartz around the periphery of quartz phenocryst in the strong alteration rocks (sericite-quartz alteration); (**B**) directional distribution of lenticular porphyritic quartz in the fragmented porphyritic granite; (**C**) porphyritic quartz, with its edges surrounded by tiny plagioclase (Pl), containing oligoclase, ZK301A, 283.5 m; (**D**) quartz phenocryst in the porphyritic granite, containing tiny oligoclase aggregates within the fissures, Zhuanzhilian ZK301A, 283.5 m; (**E**) tiny feldspar crystals and fluid inclusions along the growth zone of porphyritic quartz; (**F**) inclusions in the quartz phenocryst containing liquid-vapor two-phase aqueous inclusions and, CO_2-H_2O inclusions.

Table 1. Results of electron probe analysis on feldspar inclusions within porphyritic quartz (quoted from Xu et al. [19]).

	Results (wt %)												
Position No.	**F**	**SiO_2**	**FeO**	**K_2O**	**Na_2O**	**MgO**	**TiO_2**	**CaO**	**Al_2O_3**	**MnO**	**Total**	**Crystal Chemical Formula**	**Feldspar Type**
MZ-2-1-1	/	68.45	0.39	0.11	11.18	/	/	/	19.70	/	99.88	$(Na_{0.948}K_{0.006})_{0.954}[Al_{1.016}Si_3O_8]$	albite
MZ-2-1-2	/	68.41	0.28	0.09	11.42	/	/	0.04	19.32	/	99.56	$(Na_{0.971}K_{0.005}Ca_{0.002})_{0.978}[Al_{0.999}Si_{3.006}O_8]$	albite
MZ-2-1-3	/	67.88	0.37	0.11	11.54	0.02	/	0.04	19.05	/	99.01	$(Na_{0.989}K_{0.006}Ca_{0.002})_{0.997}[Al_{0.992}Si_{3.006}O_8]$	albite
MZ-2-1-4	/	64.85	0.13	15.78	0.42	/	/	0.02	18.70	0.03	99.97	$(K_{0.929}Na_{0.038}Ca_{0.001})_{0.968}[Al_{1.016}Si_{2.996}O_8]$	K-feldspar
MZ-2-1-5	/	65.31	0.22	15.88	0.39	/	/	0.02	18.47	/	100.29	$(K_{0.932}Na_{0.035}Ca_{0.001})_{0.968}[Al_{1.001}Si_{3.007}O_8]$	K-feldspar
MZ-2-1-7	/	68.25	0.25	0.08	11.78	/	/	0.06	19.23	/	99.79	$(Na_{1.002}K_{0.004}Ca_{0.003})1.007[Al_{0.995}Si_{3.001}O_8]$	albite
MZ-2-1-8	/	68.06	0.20	0.10	12.03	/	0.05	0.03	19.15	/	99.62	$(Na_{1.025}K_{0.006}Ca_{0.003})_{1.034}[Al_{0.992}Si_{2.997}O_8]$	albite
MZ-2-1-9	/	65.23	0.24	15.86	0.52	/	0.04	/	18.43	/	100.32	$(K_{0.931}Na_{0.046})_{0.977}[Al_{0.999}Si_{3.006}O_8]$	K-feldspar
ZK102-1	/	68.03	0.21	0.12	11.24	0.02	/	0.08	19.50	0.05	99.31	$(Na_{0.959}K_{0.007}Ca_{0.004})_{0.970}[Al_{1.001}Si_{2.998}O_8]$	albite
ZK102-2	/	64.99	/	16.05	0.23	/	/	/	18.84	/	100.21	$(K_{0.942}Na_{0.021})_{0.963}[Al_{1.021}Si_{2.994}O_8]$	K-feldspar
ZK102-3	/	68.22	0.21	0.12	11.68	/	/	/	19.42	/	99.74	$(Na_{0.993}K_{0.007})_{1.00}[Al_{1.004}Si_{2.997}O_8]$	albite
ZK102-4	/	64.75	0.06	16.02	0.63	/	0.08	/	18.10	/	99.64	$(K_{0.948}Na_{0.057})_{1.005}[Al_{0.989}Si_{3.007}O_8]$	K-feldspar
ZK102-5	/	68.35	0.10	0.13	11.87	/	0.08	0.04	19.36	/	99.93	$(Na_{1.007}K_{0.007}Ca_{0.002})_{1.016}[Al_{0.999}Si_{2.997}O_8]$	albite
ZK102-6	/	65.19	0.06	16.37	0.51	/	/	/	18.46	/	100.59	$(K_{0.959}Na_{0.045})_{1.004}[Al_{0.999}Si_{2.999}O_8]$	K-feldspar
ZK102-7	/	67.92	0.04	0.15	11.80	/	/	0.11	19.59	/	99.65	$(Na_{1.004}K_{0.008}Ca_{0.005})_{1.017}[Al_{1.013}Si_{2.985}O_8]$	albite
ZK102-8	/	64.75	0.04	16.29	0.30	/	/	0.02	18.82	/	100.26	$(K_{0.957}Na_{0.027}Ca_{0.001})_{0.986}[Al_{1.022}Si_{2.987}O_8]$	K-feldspar
ZK102-9	/	65.12	0.16	15.74	1.09	/	/	0.02	18.19	/	100.36	$(K_{0.925}Na_{0.097}Ca_{0.001})_{1.023}[Al_{0.987}Si_{3.004}O_8]$	K-feldspar
ZK102-10	/	68.55	0.18	0.16	11.93	/	/	0.03	19.33	/	100.26	$(Na_{1.010}K_{0.009}Ca_{0.001})_{1.020}[Al_{0.995}Si_{2.999}O_8]$	albite
ZK301A-248-1	/	68.24	0.31	0.20	11.31	0.02	/	0.04	19.69	/	99.84	$(Na_{0.960}K_{0.011}Ca_{0.002})_{0.973}[Al_{1.016}Si_{2.994}O_8]$	albite
ZK301A-248-2	/	64.49	/	16.25	0.33	/	/	/	19.12	/	100.19	$(K_{0.955}Na_{0.029})_{0.984}[Al_{1.038}Si_{2.975}O_8]$	K-feldspar
ZK301A-248-3	/	64.24	0.09	15.93	0.38	/	/	0.03	18.96	/	99.63	$(K_{0.941}Na_{0.034}Ca_{0.001})_{0.976}[Al_{1.035}Si_{2.980}O_8]$	K-feldspar

4. Zircon Dating

4.1. Analytical Method

Zircon particles were separated from samples of porphyritic granite using heavy liquid and magnetic techniques, and then by handpicking under a binocular microscope, at the Hebei Institute of Geological and Mineral Survey (Langfang, China), and targets was made according to Yuan et al. [20,21]. The selected zircon particles are then adhered to a double-sided tape, fixed with an epoxy resin and a curing agent amine, and ground until the zircon particles are maximally polished. To analyze their internal structures, cathodeluminescence (CL) images were obtained at Beijing Zircon Leading Technology Co., Ltd. (Beijing, China). Distinct domains within the zircon were selected for analysis, based on the CL images.

LA-ICP-MS zircon U-Pb dating of sample D35 was performed using an Agilent 7500a ICP-MS (Agilent, Santa Clara, CA, USA) equipped with a 193 nm laser, housed in the Beijing Zircon Leading Technology Co., Ltd. The room temperature was 20 °C and the relative humidity was 30%. NIST610 [22]. A reference material of synthetic silicate glass developed by American National Institute of Standards and Technology, and was used as an external standard material. Si was used as an internal standard element during elemental content analysis. During the test, the selected zircon test area was ablated using a laser beam with helium as a carrier, with a spot diameter of 30 μm and a frequency of 10 Hz. The sampling method is single point erosion, and the data acquisition needs 100s, of which the background measurement time is 40s and the signal measurement time is 60s. A zircon 91500 and a NIST 610 were measured at each of five sample sites. The ablated sample was transported to the ICP-MS using helium as a carrier, mixed with argon gas in a 30 cm^3 mixing chamber, and then ionized in a plasma, next, used the mass spectrometer to measure the isotope ratio of the ionized material, then calculated the content of the relevant element and the isotopic age of the measured mineral based on the measured results of the isotope ratio and the corresponding standard mineral. Isotope ratio data processing was performed using GLITTER (ver 4.0, Maequarie University, Sydney, Australia) software. The software in Andersen [23] was used to perform common lead corrections on test data. Age calculation and mapping were performed using ISOPLOT (ver 3.70) software [24].

4.2. Zircon Characteristics

The porphyritic granite sample D35 was used for zircon U-Pb dating. In this study, a total of 245 zircon were selected, with a grain size of 20–150 μm, and 30 sets of zircon data were obtained. Most zircon are subhedral on CL images with irregular contours and are characterized by hydrothermal alteration (Figures 5 and 6). Some zircon have a localized oscillating ring zone (Figure 5A,B and Figure 6A–C), showing magmatic zircon characteristics, which are residual of magmatic zircon. Some zircon are dark black (Figure 6D) (without cathodoluminescence), sheared (Figure 6E,F) or broken into sub-grains (Figure 6E,F), or filled in the edges (Figure 5B,D and Figure 6F) or cracks (Figure 5G,H) of the euhedral magmatic zircon as an irregular gulf-like shape with a rough surface (Figure 5C). This irregular zircon is obviously transformed by shearing and hydrothermal metasomatism, which are defined as the new hydrothermal zircon. Most zircon retain both the residual of magmatic zircon and the characteristics of hydrothermal zircon.

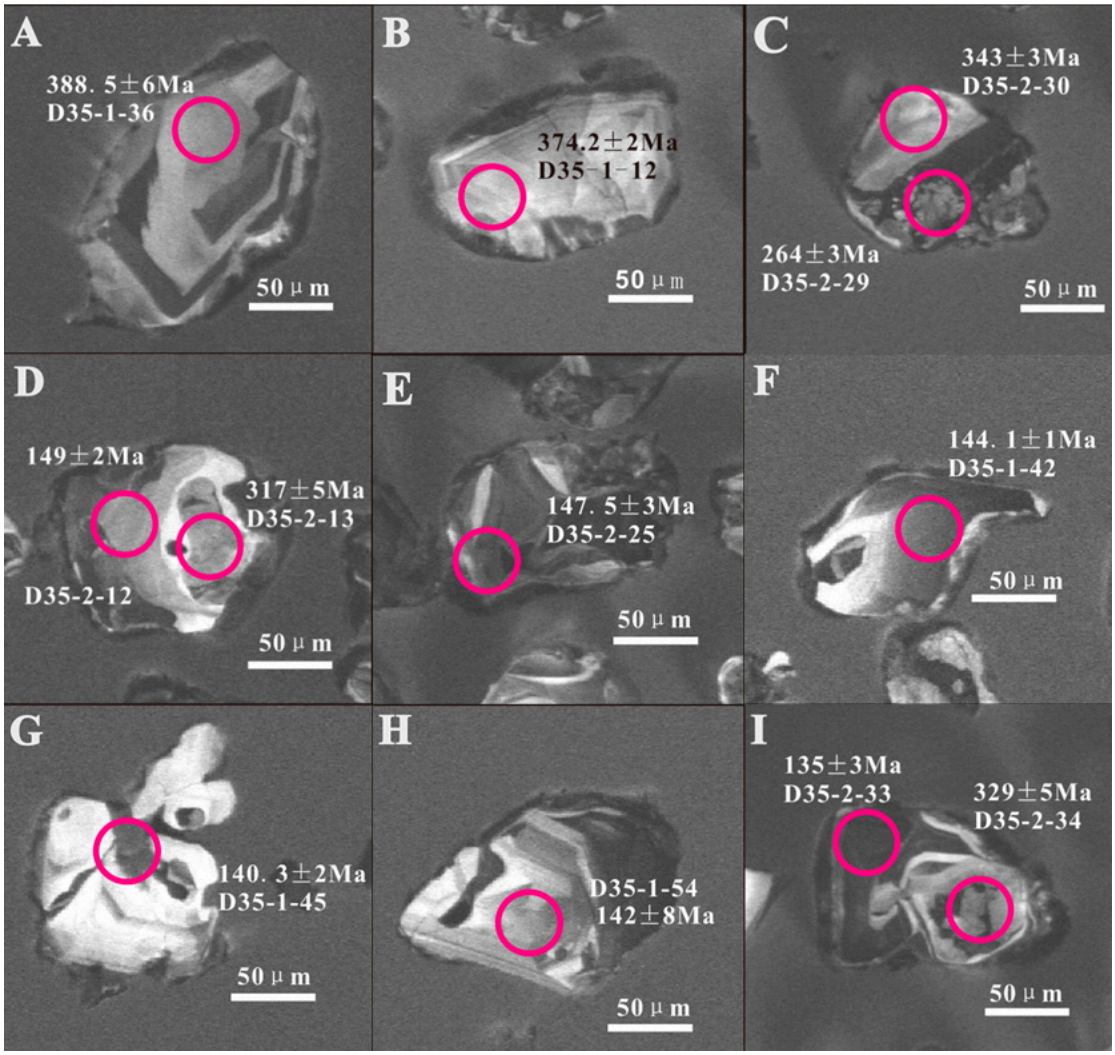

Figure 5. The measurement points on the cathodeluminescence (CL) images of zircon in porphyritic granite. (**A**) Oscillating ring zone of magmatic zircon; (**B**) weak oscillating ring zone of magmatic zircon with dark altered edge; (**C**) bright residual of magmatic zircon with rough surface below; (**D**) the magmatic zircon is transformed by the hydrothermal liquid, showing hydrothermal zircon (149 Ma) on the edge and residual of magmatic zircon (317 Ma) in the center; (**E**) dark hydrothermal zircon; (**F**) dark hydrothermal zircon with bright residual of magmatic zircon; (**G**) dark hydrothermal zircon filling along crack of magmatic zircon; (**H**) the magmatic zircon is transformed by the hydrothermal liquid, showing hydrothermal zircon in the center (142 Ma) and weak oscillating ring zone of magmatic zircon on the edge; (**I**) the magmatic zircon is transformed by the hydrothermal liquid, showing hydrothermal zircon on the edge (135 Ma) and residual of magmatic zircon (329 Ma) in the center.

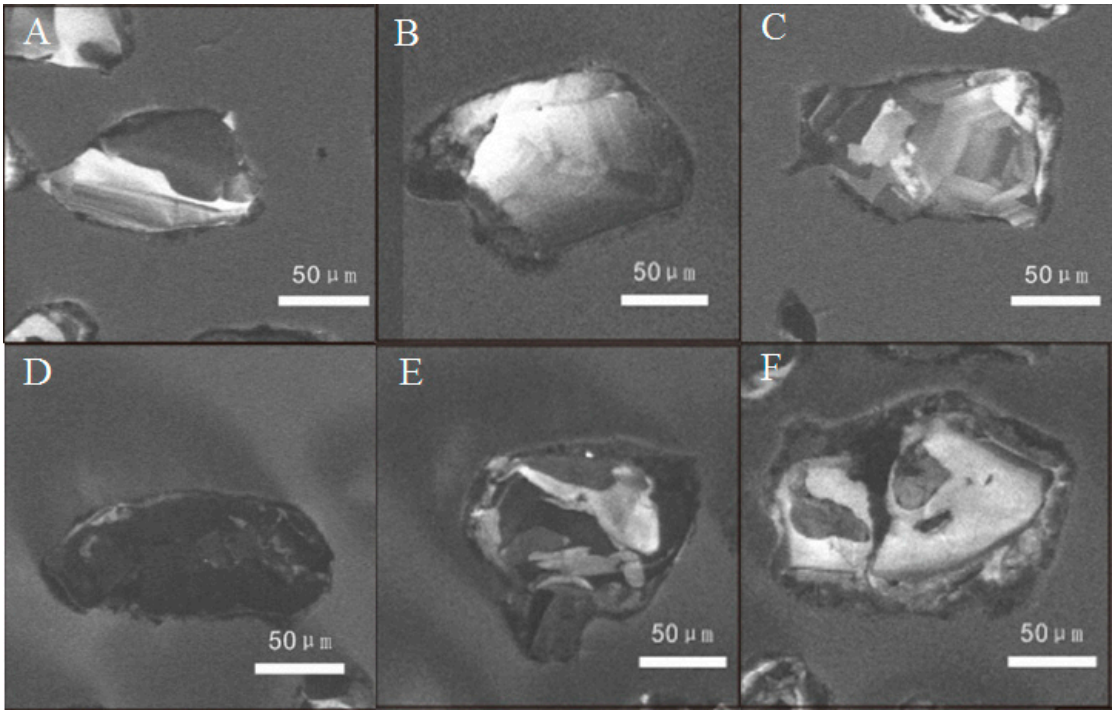

Figure 6. The CL images of zircon in porphyritic granite. (**A**–**C**) Localized oscillating ring zone of magmatic zircon; (**D**) dark hydrothermal ziron; (**E**) zircon that are sheared or broken into sub-grains; (**F**) broken magmatic zircon with altered edge.

4.3. Results

The typical results of the obtained zircon $^{206}Pb/^{238}U$, $^{207}Pb/^{235}U$, and $^{207}Pb/^{206}Pb$ values and the results of ordinary lead corrected age are shown in Table 2. Most of these measurement points are distributed on or near the U-Pb age concordant curve (Figure 7), showing good concordance. Data of zircon grains from porphyritic granite sample D35 yielded 2 groups of concordant ages at 142.02 ± 1.2 Ma (MSWD = 1.5), and 373.0 ± 3.5 Ma (MSWD = 1.5). The corresponding weighted average ages are 142.06 ± 0.84 Ma (MSWD = 1.13), and 373.0 ± 6.4 Ma (MSWD = 3.3). In general, zircon is geochemically stable by-product mineral. However, the hydrothermal fluids can replace and transform zircon to varying degrees along fractures and lattice defects within the zircon (Figure 5C,D,I and Figure 6A,F). As a result, wider alteration can occur at the edge or fissure of the zircon, resulting in the replacement of the zircon U-Pb system, and the formation of new hydrothermal zircon [25]. In spite of this, due to the stability of zircon itself, some zircon can keep the U-Pb system closed, and the U-Pb dating of zircon can still reflect geological age of primary zircon [4,5,26–28]. In the above two groups of ages, there are 8 measuring points with the old age, and there are obvious magmatic oscillation zone and bright CL images, belonging to the magmatic residual zircon [26,28–31]. This age represents the geological age of the magmatic zircon whose U-Pb system remained unreplaced, that is the age of primary magmatic zircon, which might be the age of residual zircon of Shuiquangou alkaline complex. The young zircon grains have a total of 19 sites with obvious metasomatic structures (Figure 5C,D,I and Figure 6A,F). Some grains of zircon were even converted to complete hydrothermal zircon grains (Figure 6D), which records the age of hydrothermal metasomatism, suggesting that the porphyritic granite suffered metasomatism of later hydrothermal fluid at 142.02 ± 1.2 Ma.

The rare earth element (REE) composition of magmatic and hydrothermal zircons from the porphyritic granites in Dongping Gold deposit are shown in Table 3. Hydrothermal zircon has a significantly higher REE content (Table 3). Magmatic zircon and hydrothermal zircon have distinct characteristics of rare earth patterns (Figure 8). Magma zircon increases rapidly from Pr to Lu.

The hydrothermal zircon is relatively gentle from Pr to Lu. This is consistent with typical magmatic zircon and hydrothermal zircon features.

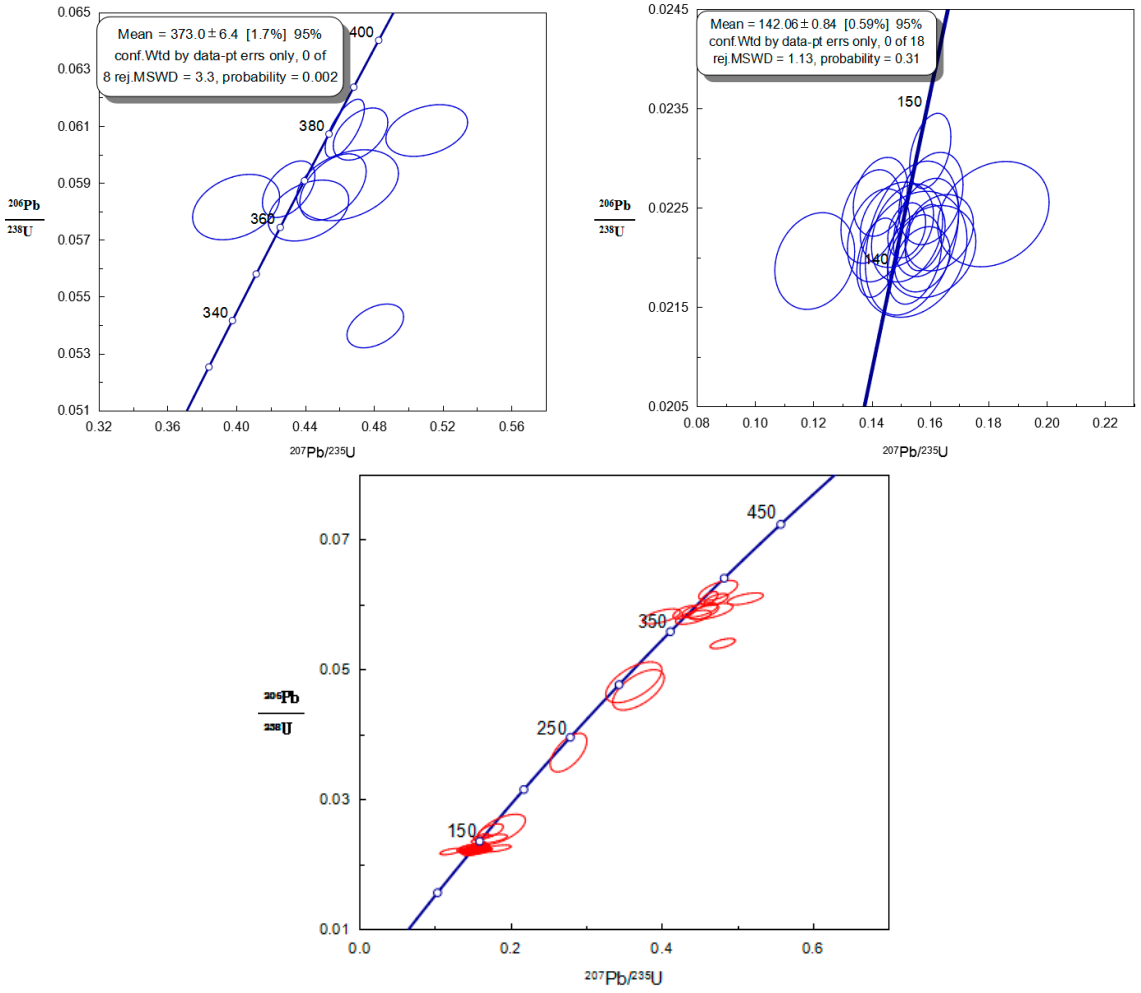

Figure 7. Concordant age diagram and weighted mean age of LA-ICP-MS zircon $^{207}Pb/^{235}U$-$^{206}Pb/^{238}U$ of porphyritic granite from Dongping deposit (D35 sample).

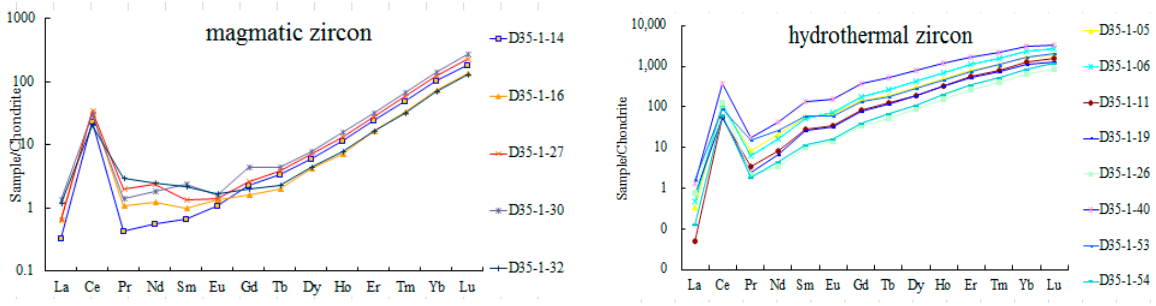

Figure 8. Chondrite-normalized REE patterns of hydrothermal, magmatic zircon.

The porphyritic granite intrudes into the monzonite of the alkaline rock along the NEE-SWW shear zone. The main elements of porphyritic granite and monzonite are shown in Table 4. Both porphyritic granite and monzonite have the characteristics of alkali-rich and high-potassium. However, the SiO_2 content of the porphyritic granite is significantly higher than that of the monzonite (Table 4).

Table 2. LA-ICP-MS zircon U-Pb dating results of porphyritic granites in Dongping gold deposit.

Measuring Point Number	Th/U	Isotope Ratio ± 1σ						Age (Ma)					
		$^{207}Pb/^{206}Pb$		$^{207}Pb/^{235}U$		$^{206}Pb/^{238}U$		$^{207}Pb/^{206}Pb$		$^{207}Pb/^{235}U$		$^{206}Pb/^{238}U$	
		Ratio	1σ	Ratio	1σ	Ratio	1σ	Age	1σ	Age	1σ	Age	1σ
D35-1-01	0.26	0.0503	0.0031	0.1538	0.0106	0.0222	0.0005	209.33	146.28	145.26	9.29	141.52	3.23
D35-1-02	0.23	0.0515	0.0040	0.1543	0.0121	0.0220	0.0004	264.88	177.76	145.71	10.64	140.49	2.64
D35-1-05	0.25	0.0534	0.0035	0.1605	0.0100	0.0221	0.0003	346.35	146.28	151.14	8.77	140.66	1.93
D35-1-06	0.28	0.0471	0.0016	0.1421	0.0048	0.0220	0.0003	53.80	77.77	134.95	4.25	140.28	1.66
D35-1-08	0.17	0.0515	0.0022	0.1603	0.0073	0.0226	0.0003	264.88	97.21	150.96	6.35	144.04	1.94
D35-1-11	0.17	0.0501	0.0027	0.1521	0.0081	0.0222	0.0003	198.23	127.76	143.78	7.10	141.85	2.05
D35-1-19	0.12	0.0516	0.0022	0.1546	0.0061	0.0220	0.0003	333.39	98.14	146.00	5.38	140.16	1.87
D35-1-25	0.39	0.0516	0.0014	0.1583	0.0045	0.0222	0.0002	333.39	61.10	149.22	3.96	141.55	1.39
D35-1-26	0.18	0.0467	0.0023	0.1424	0.0071	0.0222	0.0003	35.28	111.10	135.15	6.27	141.69	1.95
D35-1-28	0.34	0.0519	0.0021	0.1573	0.0062	0.0220	0.0002	279.69	90.73	148.36	5.48	140.17	1.37
D35-1-38	0.27	0.0521	0.0025	0.1586	0.0074	0.0223	0.0003	300.06	109.24	149.48	6.48	142.19	2.06
D35-1-41	0.18	0.0485	0.0028	0.1486	0.0083	0.0223	0.0003	124.16	129.61	140.70	7.34	142.37	1.79
D35-1-53	0.11	0.0511	0.0013	0.1558	0.0037	0.0222	0.0002	242.66	57.40	147.04	3.21	141.61	1.34
D35-1-54	0.24	0.0506	0.0033	0.1549	0.0106	0.0222	0.0003	220.44	149.98	146.22	9.28	141.65	2.17
D35-1-55	0.10	0.0531	0.0011	0.4304	0.0101	0.0588	0.0007	331.54	54.63	363.49	7.15	368.18	3.99
D35-1-14	0.02	0.0552	0.0009	0.4631	0.0075	0.0609	0.0007	420.42	35.18	386.40	5.22	381.19	4.12
D35-1-16	0.26	0.0579	0.0026	0.4647	0.0195	0.0589	0.0008	524.11	99.99	387.53	13.54	369.05	5.00
D35-1-27	0.04	0.0567	0.0018	0.4562	0.0127	0.0589	0.0008	479.67	70.36	381.63	8.88	368.65	4.69
D35-1-30	0.05	0.0555	0.0021	0.4419	0.0155	0.0580	0.0007	431.53	86.10	371.62	10.90	363.62	4.31
D35-1-31	0.02	0.0564	0.0012	0.4722	0.0105	0.0607	0.0006	477.82	48.14	392.74	7.22	379.99	3.68
D35-1-32	0.03	0.0610	0.0019	0.5108	0.0157	0.0608	0.0006	638.91	68.51	418.96	10.55	380.74	3.64
D35-1-44	0.07	0.0499	0.0021	0.3999	0.0167	0.0581	0.0008	190.82	91.65	341.55	12.11	364.36	4.62
D35-2-25	0.16	0.0508	0.0025	0.1625	0.0095	0.0231	0.0004	231.55	110.17	152.91	8.32	147.54	3.04
D35-2-30	0.21	0.0586	0.0012	0.4409	0.0209	0.0547	0.0026	553.74	50.91	370.95	14.77	343.65	16.15

Table 3. REE composition of magmatic and hydrothermal zircons from the porphyritic granites in Dongping gold deposit.

No.	D35-1-05	D35-1-06	D35-1-11	D35-1-19	D35-1-25	D35-1-28	D35-1-38	D35-1-41	D35-1-53	D35-1-54	D35-1-14	D35-1-16	D35-1-27	D35-1-30	D35-1-32
La (μg/g)	0.11	0.15	0.02	0.22	0.38	0.17	0.70	0.07	0.50	0.04	0.10	0.21	0.20	0.42	0.37
Ce (μg/g)	88.24	97.08	45.70	45.76	232.90	78.95	41.47	63.14	72.21	52.41	18.35	26.71	28.37	24.34	16.50
Pr (μg/g)	1.02	0.78	0.41	0.31	1.95	1.01	0.19	1.05	1.81	0.23	0.05	0.13	0.25	0.17	0.36
Nd (μg/g)	12.44	9.96	5.00	4.16	24.78	11.72	1.59	11.65	15.81	2.75	0.33	0.74	1.43	1.12	1.48
Sm (μg/g)	10.91	9.92	5.65	5.25	27.54	9.53	1.69	10.12	11.35	2.34	0.13	0.19	0.27	0.46	0.43
Eu (μg/g)	5.17	5.44	2.55	2.45	10.82	4.13	0.97	4.79	4.42	1.23	0.08	0.10	0.10	0.12	0.13
Gd (μg/g)	36.81	45.03	21.53	20.14	85.68	31.87	10.28	32.34	34.24	10.31	0.58	0.41	0.67	1.16	0.53
Tb (μg/g)	9.24	12.53	5.98	5.69	20.90	8.00	3.18	9.00	8.58	3.14	0.16	0.09	0.18	0.21	0.11
Dy (μg/g)	99.57	136.54	61.72	62.83	197.24	85.48	39.34	92.12	89.58	35.33	1.91	1.37	2.33	2.52	1.40
Ho (μg/g)	36.20	50.91	23.53	23.21	65.13	31.25	16.05	34.33	32.84	14.77	0.81	0.52	0.94	1.14	0.57
Er (μg/g)	164.34	232.00	115.69	109.10	255.58	141.89	75.07	153.03	150.94	71.49	5.07	3.37	5.89	6.58	3.47
Tm (μg/g)	36.31	50.06	26.21	24.10	51.07	32.99	17.10	35.44	34.71	17.29	1.59	1.07	1.85	2.14	1.01
Yb (μg/g)	341.27	481.09	263.70	226.83	452.10	316.87	164.90	336.15	357.44	178.51	21.91	15.12	26.10	29.79	14.26
Lu (μg/g)	63.48	87.22	49.54	41.87	75.60	59.09	31.24	63.17	66.33	38.98	5.86	4.36	7.28	8.57	4.03
ΣREE (μg/g)	905.11	1218.68	627.23	571.91	1501.67	812.95	403.78	846.41	880.76	428.81	56.94	54.40	75.87	78.73	44.64
δEu	0.71	0.66	0.62	0.64	0.62	0.65	0.55	0.74	0.63	0.64	0.74	1.07	0.72	0.46	0.80
δCe	24.98	35.19	33.13	35.09	33.57	22.15	27.08	17.65	10.85	63.83	58.43	37.70	26.50	21.86	9.82
Age **(Ma)**	140 ± 2	140 ± 1	141 ± 2	140 ± 2	141 ± 1	140 ± 1	142 ± 2	142 ± 2	142 ± 1	142 ± 2	381 ± 4	369 ± 5	369 ± 5	364 ± 4	380 ± 4

Table 4. Main element (wt %) analysis result.

Number	ZK102	ZK301A	MZZ-2	HTL202
Discription	**Porphyritic Granite**	**Porphyritic Granite**	**Porphyritic Granite**	**Monzonite**
SiO_2	71.39	72.40	75.54	65.06
Al_2O_3	14.78	13.75	12.92	15.31
Fe_2O_3	1.95	2.21	1.65	5.88
MgO	0.08	0.12	0.08	0.53
CaO	0.81	0.72	0.12	1.94
Na_2O	5.27	3.89	4.37	3.50
K_2O	5.35	6.51	4.91	5.56
MnO	0.05	0.06	0.02	0.08
TiO_2	0.07	0.07	0.05	0.64
P_2O_5	0.01	0.01	0.01	0.12
Ignition Loss	0.15	0.15	0.22	1.38
FeO	0.95	1.13	0.55	3.04
total	99.90	99.89	99.90	99.99
AR	5.28	6.11	5.93	3.21
A/NK	1.02	1.02	1.03	1.30
A/CNK	0.93	0.93	1.01	1.00
SI	0.56	0.87	0.68	2.85
FL	92.95	93.53	98.70	82.36
MF	97.45	96.53	96.53	94.42

A/CNK = $Al_2O_3/(CaO + Na_2O + K_2O)$; A/NK = $Al_2O_3/(Na_2O + K_2O)$; (AR) = $[Al_2O_3 + CaO + (Na_2O + K_2O)]/[Al_2O_3 + CaO - (Na_2O + K_2O)]$ (wt %); SI = $100 \times MgO/(MgO + Fe_2O_3 + FeO + Na_2O + K_2O)$ (wt %); FL = $100 \times (Na_2O + K_2O)/(CaO + Na_2O + K_2O)$ (wt %); MF = $100 \times (Fe_2O_3 + FeO)/(MgO + Fe_2O_3 + FeO)$ (wt %).

5. Discussion

5.1. Diagenetic Age and Metallogenetic Age of Porphyritic Granite

The gold-bearing porphyritic granite occurs along a NEE-SWW-striking zone with a width of 15–50 m within the Shuiquangou alkaline complex. That is, the mineralized porphyritic granite is controlled by the NEE-SWW shear zone with strong potassium enrichment and silicification. So, the age of porphyritic granite should not be much earlier than 140 Ma according to the age of the relatively open structure [13]. Therefore, the age of 373 ± 3.5 Ma may be for residual zircon of Shuiquangou alkaline complex.

In this paper, although the zircon with an average age of 373.0 ± 3.5 Ma was later replaced by hydrothermal fluids, most of the zircon showed hydrothermal zircon characteristics. However, some zircon may still retain magmatic zircon features. Therefore, it was considered that the residual zircon in the alkaline rock was trapped during emplacement of the porphyritic granite into NE-SW shear zone.

Wei et al. [16] believed that the volcanic activity of the middle-acid volcanic rocks in the Zhangjiakou Formation may provide important heat sources and ore-forming fluids for the Dongping gold deposit. The previous paper introduced there were many medium-acid rock bodies in this area at 140 Ma or so. These rock bodies can provide important heat sources and ore-forming fluids for the Dongping gold deposit. Li et al. [9] selected zircon from the potassium altered rock in the deep vein of No. 70, obtained the zircon age at the Dongping gold deposit as 140.3 ± 1.4 Ma which is the gold metallogenic age. These high-precision isotopic age results are all Early Cretaceous. Over the past decade, there have been many reports of the discovery of the hydrothermal zircon and hydrothermal zircon U-Pb dating in gold deposits [29,32]. Studies have shown that zircon can grow and crystallize directly from medium-low-temperature hydrothermal fluids [33,34]. Dubinska et al. [34] suggested that the zircon grains included two types of primary fluid inclusions containing either liquid CO_2 or aqueous solutions which were used to assign the P–T conditions of the zircon formation (270–300 °C, ca. 1 kbar). The formation temperature and pressure conditions of these hydrothermal zircon are very similar to that of gold-bearing veins. Therefore, the age of gold deposits can be determined by using the hydrothermal zircon U-Pb dating in gold-bearing altered rocks. The hydrothermal zircon age in

this study is 142.02 ± 1.2 Ma, which is almost consistent with the mineralization age of 140.3 ± 1.4 Ma obtained by Li et al. [5,9]. It is also consistent with Yanshanian mineralization explosion in the eastern China [35] and the view that there are three major metallogenic stages 200–160, 140 and 120 Ma in the Mesozoic in northern China [36]. According to the above age data, the age of gold mineralization occurred in the porphyritic granite may be 142.02 ± 1.2 Ma.

5.2. Hydrothermal Metasomatism and Gold Mineralization

In the presence of fluids, medium-low metamorphism can also cause changes in zircon structure, composition and age, and the effect of hydrothermal fluids on the zircon U-Pb systems clearly far exceeds the extent of metamorphism [5,28]. The defects formed by radioactive damage inside the zircon provide channels for the hydrothermal reforming. The hydrothermal fluids replace the zircon along the edge of the zircon crystal, cracks or lattice defects, resulting in the destruction of the U-Pb system and forming a complex zircon internal structure. Hydrothermal alteration, especially the hydrothermal action associated with ductile shear, has an important influence on the zircon U-Pb system [37].

The relatively open extensional structure was formed in the Zhangxuan area at 140 Ma or so, where underwent under plating with granulite facies metamorphism at Mesozoic [13]. The gold deposits in the Dongping area are mainly subjected to ductile shearing. Under the conditions of hydrothermal alteration, the zircon grains in the porphyritic granite may be modified. The characteristics and age of zircon in the porphyritic granite show that the formation of porphyritic quartz in porphyritic granites is related to the alteration and metasomatism of late hydrothermal fluids. Generally, chondrite-normalized REE patterns of magmatic zircon maintains a strong Ce anomaly, and the Ce anomaly of hydrothermal zircon is weak [5]. However, both types of zircon have strong Ce anomalies in Figure 8. This may be the fact that some magmatic zircon are not completely replaced by hydrothermal fluids and still retain the residual characteristics of magmatic zircon. Single porphyritic quartz aggregates are composed of one or several quartz crystals surrounded by fine recrystallized quartz, indicating that porphyritic quartz were subjected by later Si-rich hydrothermal fluids. The phenomenon of fine albite grains surrounding and tiny albite veins cutting the porphyritic quartz are also explained as metasomatism of late hydrothermal fluids. However, tiny albite and potassium feldspar occurring as stripe feldspar inclusions along the growth zones in porphyritic quartz may be resulted in trapping from early hydrothermal fluids which were rich in Na and K during porphyritic quartz initially grew. On the other hand, porphyritic granite intrudes into the monzonite of the alkaline rock along the NEE-SWW shear zone. Gold mineralization is intensive within the shear zone of the porphyritic granite intrusion, and Au reserves are estimated to be more than one tonnage. Silicification and potassiumization are relatively developed in the shear zone. The main element (Table 4) reveals that the porphyritic granite has a higher siliceous composition than the surrounding monzonite. These characteristics above suggest that the porphyritic quartz and gold mineralization in the porphyritic granite might be products of a late fluid metasomatism after emplacement of the porphyritic granite into NEE-SWW shear zone.

The porphyritic quartz may be originated from residual Si-rich magma. However, we did not see melt inclusions in porphyritic quartz as yet, indicating that the presence of residual magma could not be possible within the porphyritic granite. The homogenization temperatures of isolated liquid-vapor or vapor-liquid inclusions in porphyritic quartz of mineralizing porphyritic granite are higher than that of inclusions in gold-rich ores, which represents two hydrothermal stages [38]. Xu et al. [19] suggests that isolated liquid-vapor or vapor-liquid inclusions in the porphyritic quartz, might represent the initial fluids that later yielded gold-forming fluids. So, the tiny albite and K-feldspar along the growth belt of porphyritic quartz, might be the initial component of gold-forming fluids.

As for the source of hydrothermal fluid, in combination with age data, it might be associated with volcanic activity during the Late Jurassic−Early Cretaceous period or the evolution of small intrusions, dikes, and hidden rock masses around the ore body during the Yanshanian period. These volcanic

activities could provide heat sources and power, also produced later magmatic hydrothermal fluids, which extracted and activated part of the gold from the Shuiquangou alkaline complex. This is an important factor for the enrichment of gold in porphyritic granites, which resulted in precipitation of gold under suitable physical and rock conditions.

It can be seen from the above that the porphyritic granite and gold mineralization in the porphyritic granite might be products of a late fluid metasomatism and are controlled by the shear zone. Therefore, the porphyritic granite and NEE-SWW shear structure can be used as two prospecting indicators for gold.

6. Conclusions

A total of 30 analyses of zircon grains from porphyritic granite sample D35 yielded two groups of concordant ages at 142.0 ± 1.2 Ma (MSWD = 1.5) and 373.0 ± 3.5 Ma (MSWD = 1.5), which might represent the age of residual magma of Shuiquangou alkaline complex and metallogenetic ages of porphyritic granite respectively. Porphyritic quartz in the porphyritic granites might be related to the alteration and metasomatism of Si-rich hydrothermal fluids after emplacement of the porphyritic granite into NEE-SWW shear zone. The porphyritic quartz and gold mineralization might be products of a late fluid metasomatism. The isolated liquid-vapor or vapor-liquid inclusions and tiny albite or K-feldspar along the growth belt of porphyritic quartz, might represent the initial fluids that were rich in Na/K and later yielded gold-forming fluids.

Author Contributions: H.W. wrote the paper and performed data treatment; J.X. formulated the problem, organized the research team, guided the study, participated in writing the manuscript and revised paper; G.Z. provided natural samples and edited paper format; X.C., H.C., C.B., Z.Z. participated in experimental program.

Funding: This work is funded by National Nature Science Foundation of China (grants No. 41672070) and Doctoral Research Foundation of Hebei GEO University (No. BQ201614).

Acknowledgments: We thank the Dongping Gold Mine for its support and Zirconium for the zircon testing service. We are grateful to an anonymous reviewer and Galina Palyanova for helpful comments and suggestions.

Conflicts of Interest: The authors declare no conflict of interest.

References

1. Sillitoe, R.H. Some metallogenic features of gold and copper deposits related to alkaline rocks and consequences for exploration. *Miner. Dépos.* **2002**, *37*, 4–13. [CrossRef]
2. Müller, D. Gold-copper mineralization in alkaline rocks. *Miner. Dépos.* **2002**, *37*, 1–3. [CrossRef]
3. Zhu, Y.P.; Zhao, X.D.; Tan, G.L.; Yao, Z.Y.; Zhao, Y.H. Metallogenetic characteristics of Cadia-Ridgeway Porphyry Gold-Copper Deposit in Australia. *West. China Sci. Technol.* **2015**, *14*, 24–29.
4. Luo, Z.K.; Miao, L.C.; Guan, K. SHRIMP geochronology of the Shuiquangou rock mass and its significance in Zhangjiakou. *Hebei Geochem.* **2001**, *30*, 116–122.
5. Li, C.M.; Deng, J.F.; Chen, L.H. Constraint from two stages of zircon on the metallogenic age in the Dongping gold deposit, Zhangxuan area, northern North China. *Miner. Depos. Geol.* **2010**, *29*, 265–275.
6. Xiang, S.Y.; Ye, J.L.; Liu, J. The origin of alkaline syenite in Hougou gold deposit and its relationship with gold mineralization. *Mod. Geol.* **1992**, *6*, 55–62.
7. Song, G.R.; Zhao, Z.H. *Geological Geology of the Dongping Alkaline Complex in Hebei Province*; Seismological Press: Beijing, China, 1996; pp. 1–181.
8. Li, H.M.; Li, H.K.; Lu, S.N.; Yang, C.L. Using the U-Pb dating of hydrothermal zircon in ore veins to determine the metallogenic age of Dongping gold deposit. *Earth J.* **1997**, *18*, 176–178.
9. Li, C.M.; Deng, J.F.; Su, S.G.; Li, H.M.; Liu, X.M. Two-stage zircon chronology and its significance in potash altered rocks in Dongping Gold deposit, Hebei Province. *J. Earth Sci.* **2010**, *31*, 843–852.
10. Mo, C.H.; Wang, X.Z.; Liang, H.Y. The U-Pb ages and their geological significance of Shangshuiquan granites in the Dongping gold deposit. *J. Mineral.* **1998**, *18*, 298–301.
11. Jiang, S.H.; Nie, F.J. The ^{40}Ar-^{39}Ar isotopic geochronology of the Shuiquangou Complex and its related gold deposits in Northwest Yunnan. *Geol. Forum* **2000**, *46*, 621–627.

12. Nie, F.J.; Jiang, S.H.; Liu, Y. Intrusion-related gold deposits of North China Craton, People's Republic of China. *Resour. Geol.* **2004**, *54*, 299–324. [CrossRef]
13. Shao, J.A.; Wei, C.J.; Zhang, L.Q.; Niu, S.Y.; Mou, B.L. Pyroxene diorite in nuclear department of Zhangxuan Uplift. *Acta Petrol. Sin.* **2004**, *20*, 1389–1396.
14. Liu, B. Metallogenic characteristics of alkaline intrusive complexes in Hougou, Shuiquangou, Northern Hebei Province. *Geol. Resour.* **2001**, *10*, 25–32.
15. Li, C.M. *Study on Chronology and Petrochemistry in Dongping and Hougou Gold Orefields, Northern Hebei Province*; China University of Geoscience: Beijing, China, 2011.
16. Wei, Z.L.; Zhang, H.; Liu, X.M.; Zhang, Y.Q. LA-ICP-MS dating of volcanic rocks in Zhangjiakou Formation, Zhangjiakou area and its geological significance. *Prog. Nat. Sci.* **2008**, *18*, 523–530.
17. Jiang, N.; Zang, S.Q.; Zhou, W.G.; Liu, Y.S. Origin of a Mesozoic granite with A-type characteristics from the North China craton: Highly fractionated from I-type magmas? *Contrib. Mineral. Petrol.* **2009**, *158*, 113–130. [CrossRef]
18. Jiang, N.; Liu, Y.S.; Zhou, W.G.; Yang, J.H.; Zhang, S.Q. Derivation of Mesozoic adakitic magmas from ancient lower crust in the North China craton. *Geochim. Cosmochim. Acta* **2007**, *71*, 2591–2608. [CrossRef]
19. Xu, J.H.; Wand, Y.W.; Bian, C.J.; Zhang, G.R.; Chu, H.X. Unusual quartz phenocrysts in a newly discovered porphyritic granite near the giant Dongping Gold Deposit in Northern Hebei Province, China. *Acta Geol. Sin.* **2018**, *92*, 398–399. [CrossRef]
20. Yuan, H.L.; Gao, S.; Dai, M.N.; Zong, C.L.; Detlef, G.; Gisela, H.F.; Liu, X.M.; Diwu, C.R. Simultaneous determinations of U-Pb age, Hf isotopes and trace element compositions of zircon by excimer laser-ablation quadrupole and multiple-collector ICP-MS. *Chem. Geol.* **2008**, *247*, 100–118. [CrossRef]
21. Yuan, H.; Wu, F.; Gao, S.; Liu, X.; Xu, P.; Sun, D. Determination of U-Pb age and rare earth element concentrations of zircons from Cenozoic intrusions in northeastern China by laser ablation ICP-MS. *Chin. Sci. Bull.* **2003**, *48*, 2411–2421.
22. Pearce NJ, G.; Perkins, W.T.; Westgate, J.A.; Gorton, M.P.; Jackson, S.E.; Neal, C.R.; Chenery, S.P. A compilation of new and published major and trace element data for NIST SRM 610 and NIST SRM 612 glass reference materials. *Geostand. Newsl.* **1997**, *21*, 115–144. [CrossRef]
23. Andersen, T. Correction of common Pb in U-Pb analyses that do not report ^{204}Pb. *Chem. Geol.* **2002**, *192*, 59–79. [CrossRef]
24. Ludwig, K.R. *User's Manual for Isoplot 3.70: A Geochronological Toolkit for Microsoft Excel*; Special Publication No. 4; Berkeley Geochronology Center: Berkeley, CA, USA, 2008; Volume 76.
25. Kroner, A.; Jaeckel, P.; Williams, I.S. Pb-loss patterns in zircons from a high-grade metamorphic terrain as revealed by different dating methods: U-Pb and Pb-Pb ages of igneous and metamorphic zircon from northern Sri Lanka. *Precambrian Res.* **1994**, *66*, 151–181. [CrossRef]
26. Liati, A.; Gebauer, D.; Wysoczanski, R. U-Pb SHRIMP dating of zircon domains from UHP garnet-rich mafic rocks and late pegmatoids in the Rhodope zone (N Greece): Evidence for Early Cretaceous crystallization and Late Cretaceous metamorphism. *Chem. Geol.* **2002**, *184*, 281–299. [CrossRef]
27. Tomaschek, F.; Kennedy, A.K.; Villa, I.M. Zircons from Syros, Cyclades, Greece-recrystallization and mobilization of zircon during high-pressure metamorphism. *J. Petrol.* **2003**, *44*, 1977–2002. [CrossRef]
28. Li, C.M. Review on zircon genetic mineralogy and zircon micro area dating. *Geol. Surv. Res.* **2009**, *33*, 161–174.
29. Hu, F.F.; Fan, H.R.; Yang, J.H.; Wan, Y.S.; Liu, D.Y.; Zhai, M.G.; Jin, C.W. Mineralizing age of the Rushan lode gold deposit in the Jiaodong Peninsula: SHRIMP U-Pb dating on hydrothermal zircon. *Chin. Sci. Bull.* **2004**, *49*, 1629–1636. [CrossRef]
30. Liu, F.; Li, Y.H.; Mao, J.W.; Yand, F.Q.; Chai, F.M.; Mou, X.X.; Yang, Z.X. Zircon SHRIMP ages and their geological significance in the Abba granites of the Altai Orogenic Belt. *Earth J.* **2008**, *29*, 795–804.
31. Nie, F.J.; Xu, D.Q.; Jiang, S.H.; Hu, P. SHRIMP age of the zircons from the K-feldstolite in the Su-Cha fluorite deposit and its geological significance. *J. Earth Sci.* **2009**, *30*, 803–811.
32. Fu, B.; Terrence, P.M.; Noriko, T.K.; Anthony IS, K.; John, W.V. Distinguishing magmatic zircon from hydrothermal zircon: A case study from the Gidginbung high-sulphidation Au-Ag-(Cu) deposit, SE Australia. *Chem. Geol.* **2009**, *259*, 131–142. [CrossRef]
33. Cherniak, D.J.; Watson, E.B. Diffusion in zircon. *Rev. Mineral. Geochem.* **2003**, *53*, 113–143. [CrossRef]
34. Dubinska, E.; Bylina, P.; Kozlowski, A. U-Pb dating of serpentinization: Hydrothermal zircon from a metasomatic rodingite shell (Sudetic ophiolite, SW Poland). *Chem. Geol.* **2004**, *203*, 183–203. [CrossRef]

35. Deng, J.F.; Mo, X.X.; Zhao, H.L.; Luo, Z.H.; Zhao, G.C.; Dai, S.Q. Catastrophic lithosphere and asthenosphere system in eastern China during the Yanshanian period. *Miner. Depos. Geol.* **1999**, *18*, 309–315.
36. Mao, J.W.; Xie, G.Q.; Zhang, Z.H.; Li, X.F.; Wang, Y.T.; Zhang, C.Q.; Li, Y.F. Mesozoic large-scale mineralization and its geodynamic setting in northern China. *Acta Petrol. Sin.* **2005**, *21*, 170–188.
37. Bao, Z.W.; Zhao, Z.H. Effect of Hydrothermal Alteration on Zircon, U-Pb Dating. In Proceedings of the National Symposium on Petrology and Geodynamic, Nanjing, China, 1−6 November 2006.
38. Zhang, G.R.; Xu, J.H.; Wei, H.; Song, G.C.; Zhang, Y.B.; Zhao, J.K.; He, B.; Chen, D.L. Structure, alteration, and fluid inclusion study on deep and surrounding area of the Dongping gold deposit, Northern Hebei, China. *Acta Petrol. Sin.* **2012**, *28*, 637–651.